NEUROSCIENCE

Serotonin release in the habenula during emotional contagion promotes resilience

Sarah Mondoloni[1], Patricia Molina[1], Salvatore Lecca[1], Cheng-Hsi Wu[1], Léo Michel[1], Denys Osypenko[1], Fanchon Cachin[1]†, Meghan Flanigan[2], Mauro Congiu[1], Arnaud L. Lalive[1], Thomas Kash[2], Fei Deng[3], Yulong Li[3], Manuel Mameli[1,4]*

Negative emotional contagion—witnessing others in distress—affects an individual's emotional responsivity. However, whether it shapes coping strategies when facing future threats remains unknown. We found that mice that briefly observe a conspecific being harmed become resilient, withstanding behavioral despair after an adverse experience. Photometric recordings during negative emotional contagion revealed increased serotonin (5-HT) release in the lateral habenula. Whereas 5-HT and emotional contagion reduced habenular burst firing, limiting 5-HT synthesis prevented burst plasticity. Enhancing raphe-to-habenula 5-HT was sufficient to recapitulate resilience. In contrast, reducing 5-HT release in the habenula made witnessing a conspecific in distress ineffective to promote the resilient phenotype after adversity. These findings reveal that 5-HT supports vicarious emotions and leads to resilience by tuning definite patterns of habenular neuronal activity.

The capacity of humans and rodents to cope with adversity suggests the harnessing of resilience as a strategy to reduce trauma vulnerability, but how to promote this protective phenotype remains a challenge (*1*–*4*). Observing others in adverse circumstances [referred to as negative emotional contagion (NEC)] shields individuals from direct traumatic experiences (*5*). Yet, this vicariously triggers an emotional state that facilitates the extraction of relevant information about potential future threats (*6*–*9*). Wi… the brain, the lateral habenula (LHb) enc… threats but also adversity-driven negative affect through excessive neuronal bursting (*10*, *11*). However, it remains elusive whether emotional contagion adjusts an individual's affective state to produce resilience and whether habenular mechanisms underlie these processes.

NEC promotes resilience

To examine the behavioral relevance of vicarious emotions, we used a task wherein mice [bystanders (BY)] experienced NEC (see methods in the supplementary materials; Fig. 1A). Here, mice observed a cage mate (demonstrator) submitted to a harmful experience (one session of 19 foot shocks over the course of 20 min). Control mice spent a similar amount of time in the apparatus while observing a nonshocked conspecific. To assess whether NEC is effective in changing the emotional responsivity of bystanders, we quantified distinct behavioral signatures. During the task, bystanders exhibited movement arrest (longer pause duration) and displayed interest in the demonstrator, as indicated by the more frequent nose pokes of the floor (investigation), compared with

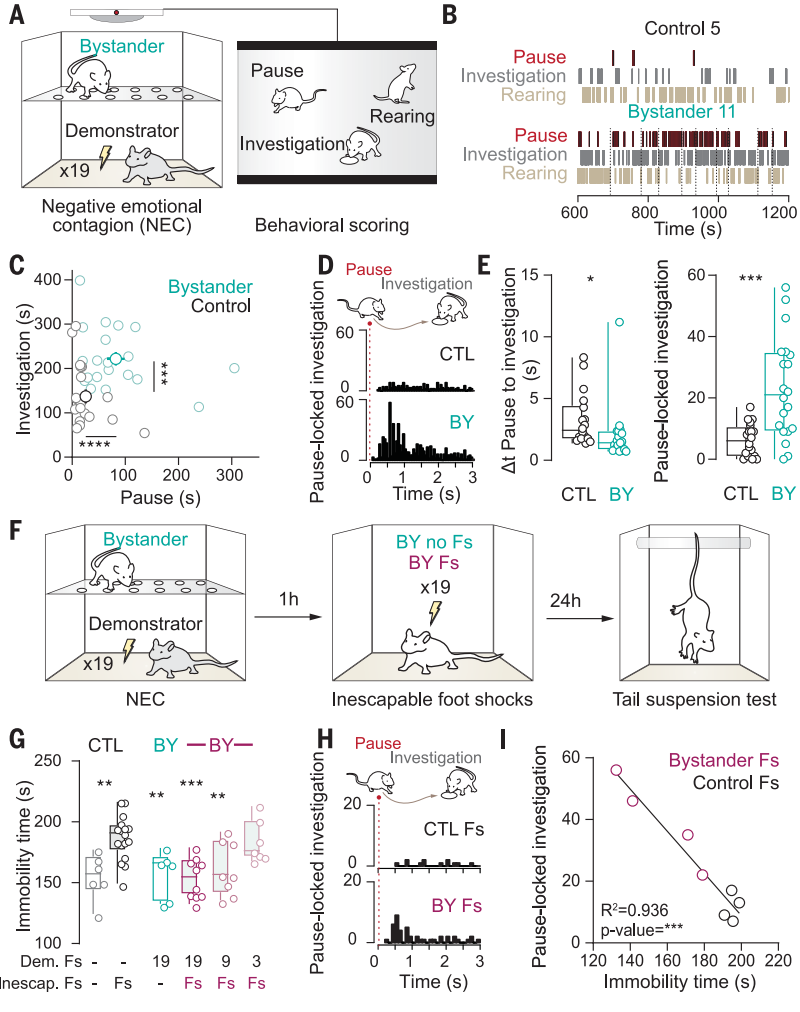

Fig. 1. Negative emotional contagion promotes resilience. (**A**) Schematic of the NEC paradigm. (**B**) Time stamp of pause, investigation, and rearing behaviors during NEC for a control mouse and a bystander mouse. Dashed lines indicate foot shocks on demonstrator. (**C**) Investigation and pause cumulative time per mouse during NEC (Mann-Whitney test, n_{CTL} = 20, n_{BY} = 20, P_{pause} < 0.0001, $P_{investigation}$ = 0.0004). (**D**) Investigation events after pause instances in control (CTL) and bystander (BY). (**E**) Pause-to-investigation delay and pause-locked investigation in controls and bystanders (Mann-Whitney test, n_{CTL} = 20, n_{BY} = 20, P_{delta} = 0.0029, P_{events} = 0.0002). (**F**) Schematic of the experimental settings. Fs, foot shocks. (**G**) Immobility time during TST in controls and bystanders submitted or not submitted to foot shocks [$n_{CTLnoFs}$ = 6, n_{BYnoFs} = 6, n_{CTLFs} = 17, $n_{BYFs\text{-}19demFs}$ = 10, $n_{BYFs\text{-}9demFs}$ = 7, $n_{BYFs\text{-}3demFs}$ = 8, one-way analysis of variance (ANOVA); immobility time × Fs interaction, $F_{5,48}$ = 7.060, P < 0.0001]. "Dem. Fs" and "Inescap. Fs" values indicate the number of foot shocks delivered to demonstrators and controls or bystanders, respectively. (**H**) Single-mouse investigation events after pause instances in control and bystander. (**I**) Relationship between pause-to-investigation events and TST immobility time in controls and bystanders that received foot shocks [linear regression, n = 8 mice, coefficient of determination (R^2) = 0.9365, P < 0.0001]. Error bars represent mean ± SEM or median ± minimum-to-maximum (min-to-max) whiskers.

[1]The Department of Fundamental Neuroscience, The University of Lausanne, 1005 Lausanne, Switzerland. [2]The Bowles Center for Alcohol Studies, The University of North Carolina School of Medicine, Chapel Hill, NC 27599, USA. [3]State Key Laboratory of Membrane Biology, School of Life Sciences, Peking University, Beijing 100871, China. [4]Inserm, UMR-S 839, 75005 Paris, France.
***Corresponding author. Email: manuel.mameli@unil.ch**
†Present address: The Department of Neuroscience, Norwegian University of Science and Technology, 7491 Trondheim, Norway.

control mice (Fig. 1, B and C, and fig. S1, A to C). Pause and investigation were sequentially structured, which was not the case for rearing events (i.e., actions unrelated to the demonstrator) (Fig. 1, D and E, and fig. S1, D to G). Pause, investigation, and rearing were similar between bystanders and control mice before the vicarious experience (fig. S1C). Furthermore, bystanders' locomotion, sociability, behavioral reactivity to foot shocks, and despair [measured as the immobility time in a tail suspension test (TST)] remained comparable to controls after NEC (Fig. 1G and fig. S2, A to E). To understand whether NEC modulation of the individuals' affective state shapes the behavioral responses to future challenges, bystander and control mice were next exposed to an aversive paradigm known to generate depressive-like symptoms (i.e., behavioral despair; Fig. 1F) (*12*). Control mice remained immobilized for longer during a TST—a sign of despair—after receiving a series of foot shocks (one session of 19 foot shocks over the course of 20 min) (*12*, *13*). The immobility of bystander mice, on the other hand, remained comparable to that of the nonshocked counterpart (Fig. 1G). Such a resilient phenotype lasted up to 7 days, scaled up relatively to the foot shocks experienced by demonstrators, emerged in both male and female mice, and was equally observed using the novelty-suppressed feeding test (Fig. 1G and fig. S2, F and G). The immobility time observed during the TST correlated with the pause-to-investigation transitions (Fig. 1, H and I), supporting a relationship between the behavioral features emerging during NEC and the subsequent resilience. In contrast, pause-to-rearing transitions during NEC did not relate to immobility, indicating that phenotypes disconnected from NEC (rearing) are also unrelated to despair (Fig. 1, H and I, and fig. S2, H and I). Altogether, these findings indicate that NEC promotes resilience in mice.

Serotonin release in the habenula during NEC

We then explored the neural circuit mechanisms underlying the resilient phenotype. Serotonin (5-HT) release and reuptake contribute to aspects of vulnerability and resilience to trauma, profoundly shaping the individual affective state (*3*). In turn, hyperactivity of the LHb underlies susceptibility to a depressive-like phenotype (*10*). Serotonergic innervation within the LHb stems from neurons located in the raphe nucleus (both the median and dorsal territories), and exogenous 5-HT application in the LHb modulates neuronal activity and neurotransmission (*14*–*19*). However, little is known about 5-HT release dynamics within the LHb or their functional and behavioral relevance. We virally expressed a biosensor enabling 5-HT release detection in the LHb

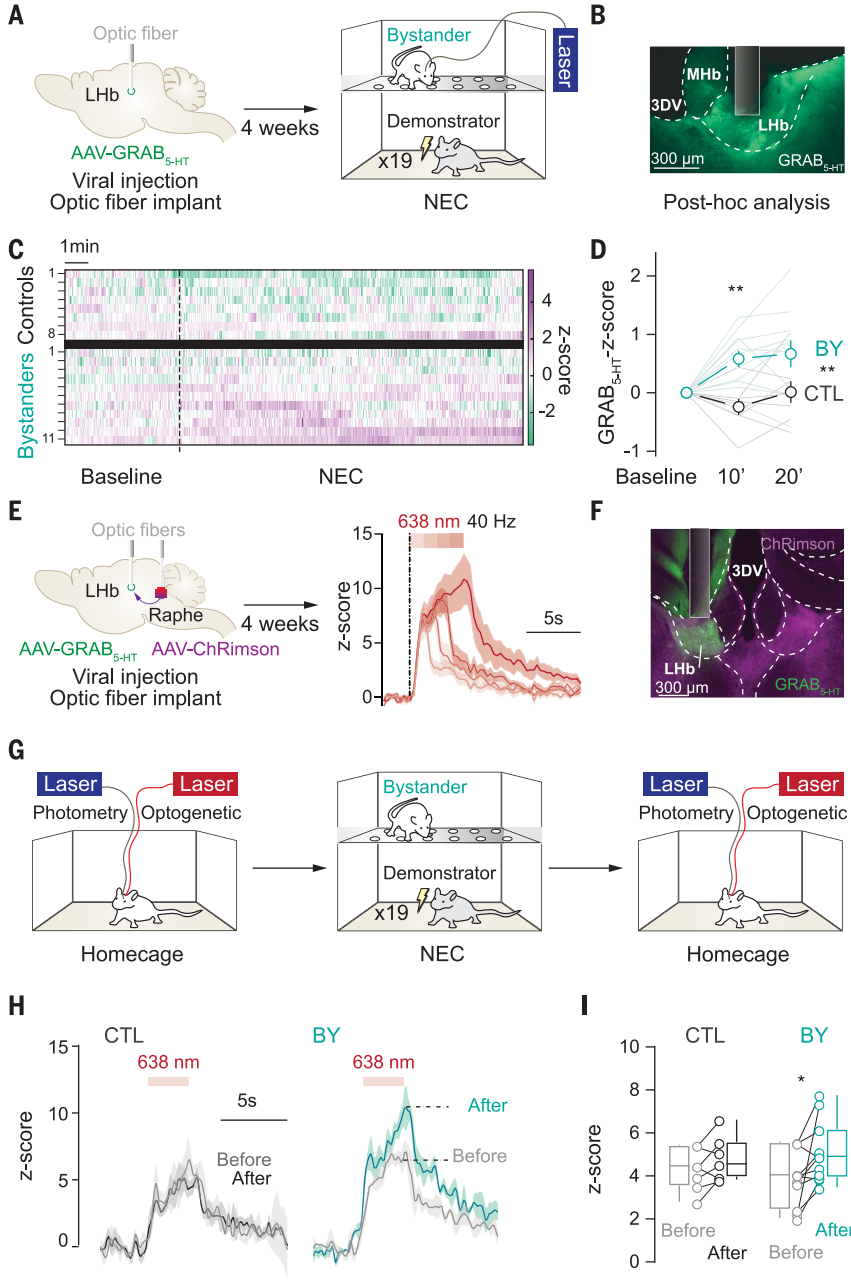

Fig. 2. 5-HT release in the LHb during NEC. (**A**) Experimental protocol. (**B**) Fiber optic placement and $GRAB_{5\text{-}HT}$ expression in the LHb. 3DV, third dorsal ventricle; MHb, medial habenula. (**C**) Heatmap *z*-score of $GRAB_{5\text{-}HT}$ dynamics of all controls and bystanders during NEC (5 min baseline and 15 min of NEC). (**D**) Average of 10-min *z*-score of $GRAB_{5\text{-}HT}$ dynamics (n_{CTL} = 8, n_{BY} = 11, two-way repeated measures ANOVA; interaction effect, $F_{2,34}$ = 5.894, P = 0.0063, with Holm-Šídák post hoc test). (**E**) Experimental protocol and light-evoked 5-HT transients in the LHb after somatic activation of raphe neurons. (**F**) Fiber optic placement, $GRAB_{5\text{-}HT}$, and ChRimson terminal expression in the LHb. (**G**) Experimental protocol. (**H**) Example *z*-score of $GRAB_{5\text{-}HT}$ dynamics after light stimulation in the raphe in control and bystander. (**I**) Quantification of $GRAB_{5\text{-}HT}$ dynamics before and after NEC (n_{CTL} = 7, n_{BY} = 11, two-way repeated measures ANOVA; time effect, $F_{1,16}$ = 7.287, P = 0.0158, with Holm-Šídák post hoc test). Error bars represent mean ± SEM or median ± min-to-max whiskers.

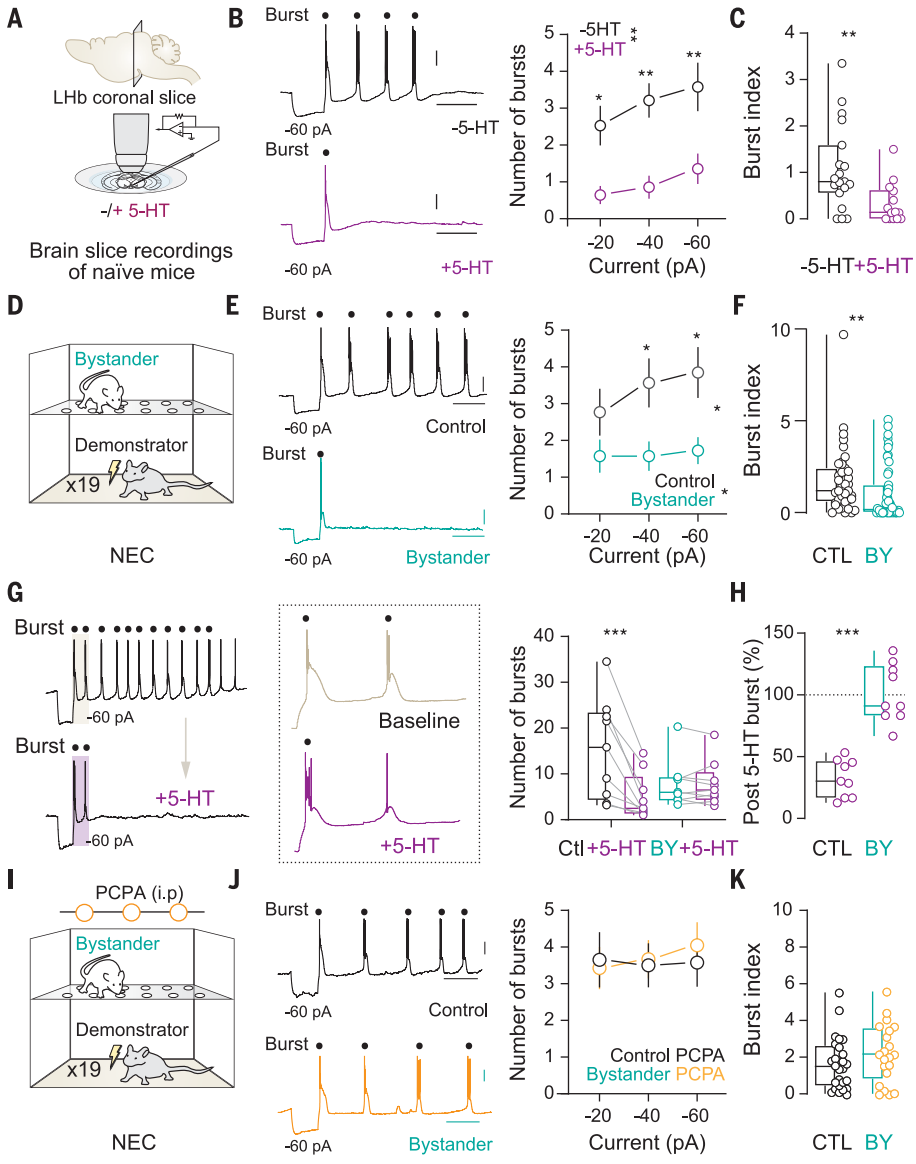

Fig. 3. 5-HT and NEC diminish LHb burst firing. (**A**) Schematic of recordings. (**B**) Bursts induced by hyperpolarization and quantification (−20, −40, and −60 pA for 0.8 s, $n_{-5\text{-HT}} = 19$, $n_{+5\text{-HT}} = 14$, two-way repeated measures ANOVA; 5-HT effect, $F_{1,31} = 10.97$, $P = 0.0024$, with Holm-Šídák post hoc test). (**C**) Burst index of LHb neurons in the presence or absence of 5-HT (Mann-Whitney test, $n_{-5\text{-HT}} = 19$, $n_{+5\text{-HT}} = 14$, $P = 0.006$). (**D**) Schematic of NEC. (**E**) Burst induced by hyperpolarization in controls and bystanders. Number of bursts induced by hyperpolarization (−20, −40, and −60 pA for 0.8 s, $n_{CTL} = 39$, $n_{BY} = 47$, two-way repeated measures ANOVA; current × NEC interaction, $F_{2,168} = 4.501$, $P = 0.0125$, with Holm-Šídák post hoc test). (**F**) Burst index in controls and bystanders (Mann-Whitney test, $n_{CTL} = 39$, $n_{BY} = 47$, $P = 0.0031$). (**G**) Example trace of LHb burst before and after 5-HT and number of bursts induced by hyperpolarization (−60 pA for 0.8 s) in controls and bystanders (two-way repeated measures ANOVA, $n_{CTL} = 9$, $n_{BY} = 9$: 5-HT × NEC interaction, $F_{2,16} = 17.49$, $P = 0.0007$, with Holm-Šídák post hoc test). (**H**) Percent change of burst induced by hyperpolarization after 5-HT bath application (Mann-Whitney test, $n_{CTL} = 9$, $n_{BY} = 9$, $P < 0.0001$). (**I**) Experimental protocol with PCPA (three intraperitoneal injections the day before NEC). (**J**) Example of burst induced by hyperpolarization in LHb slice of control PCPA and bystander injected with PCPA. Number of bursts induced by hyperpolarization (−20, −40, and −60 pA for 0.8 s, two-way repeated measures ANOVA, $n_{CTL} = 26$, $n_{BY} = 21$; current × group effect, $F_{2,90} = 1.53$, $P = 0.2211$, with Holm-Šídák post hoc test). (**K**) Burst index of LHb neurons in control and bystander mice (Mann-Whitney test, $n_{CTL} = 26$, $n_{BY} = 21$, $P = 0.24$). Error bars represent mean ± SEM or median ± min-to-max whiskers.

($GRAB_{5\text{-HT}}$; Fig. 2, A and B, and fig. S3, A and B) (*20*). Tonic $GRAB_{5\text{-HT}}$ fluorescence increased in bystanders across NEC compared with controls (Fig. 2, C and D, and fig. S3C). $GRAB_{5\text{-HT}}$ transients were time-locked with investigation bouts but not pause and rearing, supporting a relationship between behavioral features emerging during NEC and 5-HT release (fig. S2D). To corroborate these observations, we virally expressed the red-shifted opsin ChRimson in the raphe to optically evoke 5-HT release, concomitantly with the $GRAB_{5\text{-HT}}$ sensor in the LHb (Fig. 2, E and F, and fig. S3, E and F). Increasing light-pulse duration at 638 nm through a fiber optic in the raphe produced increasingly larger $GRAB_{5\text{-HT}}$ transients in the LHb, which is indicative of tunable 5-HT release (Fig. 2E). We then quantified 5-HT release before and after NEC in both control and bystander mice. In line with increased 5-HT release in the LHb during NEC, we observed larger light-evoked 5-HT transients after NEC in bystanders but not in controls (Fig. 2, H and I).

5-HT and NEC diminish LHb burst firing

Different modalities of neuronal firing (single-spike and bursting) are features of LHb neurons (*10*). Notably, enhanced LHb neuronal bursting is a hallmark of behavioral despair emerging in response to adverse conditions (*21*). If NEC limits behavioral despair by promoting resilience and increases 5-HT release in the LHb, we postulated that NEC and 5-HT would similarly diminish neuronal bursting. We examined neuronal firing at baseline and neuronal excitability. Additionally, bursting activity was quantified at baseline, during depolarization, and after a series of hyperpolarizing pulses (Fig. 3, A and B, and fig. S4, A to E). We computed a burst index for each neuron as the combined capacity of bursting during baseline and in response to positive and negative current injections, allowing us to classify bursting and nonbursting neurons (see methods). Current-clamp recordings in acute slices revealed that 5-HT (1 μM) reduced bursting of LHb neurons without affecting regular neuronal firing (Fig. 3, A to C, and fig. S4, A to F). Enhancing extracellular 5-HT levels with citalopram (10 mg/kg, injected intraperitoneally) diminished LHb bursting (fig. S4, G and I). Similarly, bystander mice showed burst reduction (both ex vivo and in vivo) and a decreased fraction of neurons bursting and burst index but unaltered excitability or resting membrane potential (Fig. 3, D to F, and fig. S5, A to J). 5-HT bath application failed to further reduce burst firing in LHb neurons from bystander mice, indicative of occlusion of this form of plasticity (Fig. 3, G and H, and fig. S5, E to G). Finally, pharmacologically depleting 5-HT by inhibiting tryptophan hydroxylase with

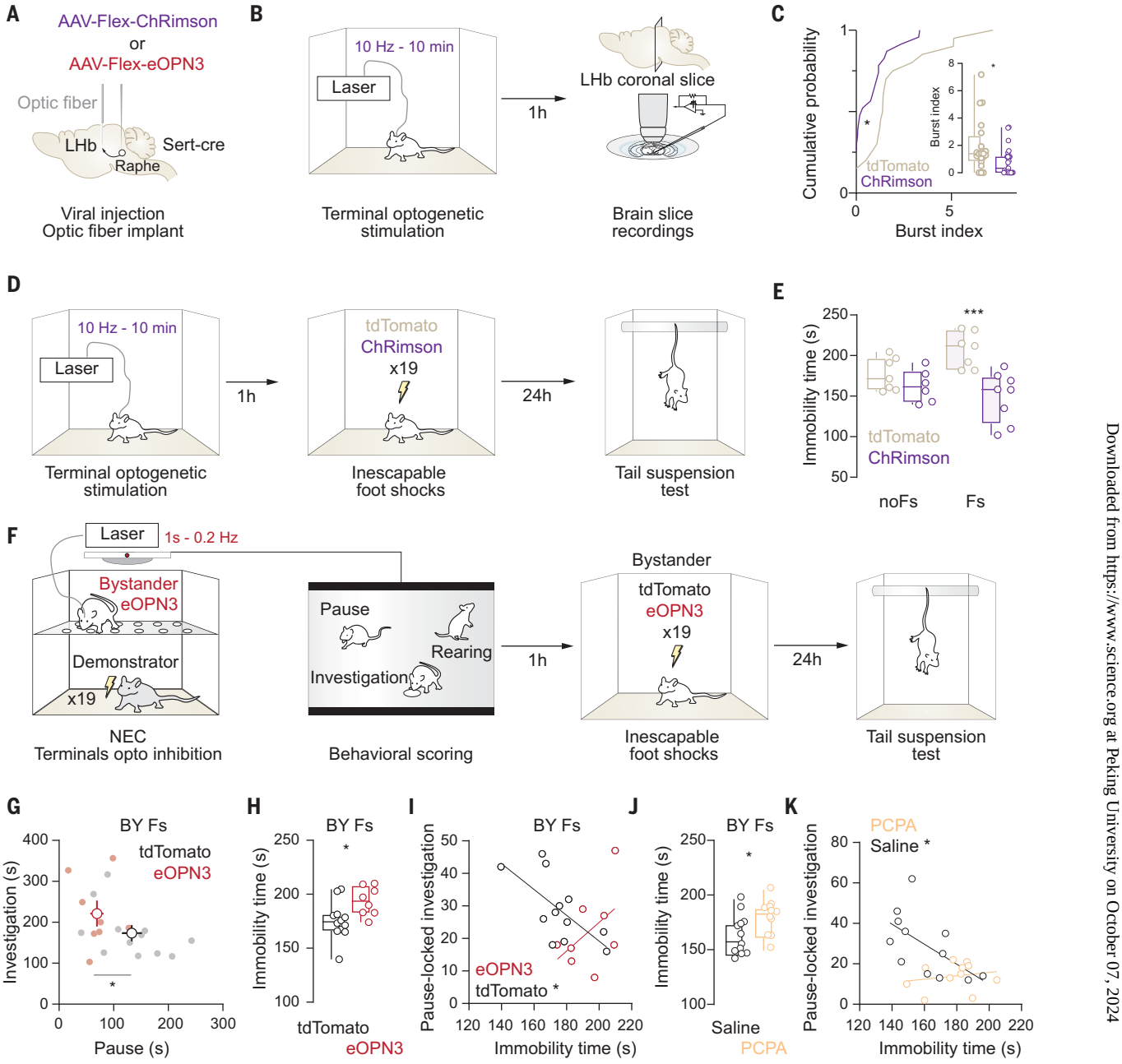

Fig. 4. Modulation of behavioral despair by 5-HT manipulation. (**A**) Schematic of surgery. (**B**) Serotonin optogenetic terminal activation before brain slice recordings. (**C**) Burst index of LHb neurons in 5-HT^{tdTomato} and 5-HT^{ChRimson} mice (Mann-Whitney, $n_{tdTomato}$ = 20, $n_{ChRimson}$ = 23, P = 0.026). (**D**) Schematic of optogenetic terminal manipulation before mice received 0 or 19 foot shocks (no Fs and Fs, respectively) and performed the TST. (**E**) Immobility time of 5-HT^{tdTomato} and 5-HT^{ChRimson} mice in no Fs or Fs condition (two-way ANOVA, $n_{tdTomato\text{-}noFs}$ = 7, $n_{ChRimson\text{-}noFs}$ = 7, $n_{tdTomato\text{-}Fs}$ = 7, $n_{ChRimson\text{-}noFs}$ = 8; immobility time × Fs interaction, $F_{1,24}$ = 5.500, P = 0.0276, with Holm-Šídák post hoc test). (**F**) Schematic of 5-HT optogenetic terminals inhibition in the LHb during NEC before receiving 19 foot shocks and performing the TST. (**G**) Investigation and pause cumulative time per mouse during NEC ($n_{tdTomato}$ = 8, n_{eOPN3} = 12, Mann-Whitney, $P_{invest.}$ = 0.115, Student's t test, P_{pause} = 0.0142). (**H**) Immobility time during the TST (Student's t test, P = 0.0211). (**I**) Relationship between pause-to-investigation events and TST immobility time in bystanders that received foot shocks (linear regression, $n_{tdTomato}$ = 8, n_{eOPN3} = 12, 5-HT^{tdTomato} R^2 = 0.4511, P = 0.0168, 5-HT^{eOPN3} R^2 = 0.2317, P = 0.2271). (**J**) Immobility time during the TST ($n_{BYFs\text{-}saline}$ = 12, $n_{BYFs\text{-}PCPA}$ = 11, Student's t test, P = 0.0287). (**K**) Relationship between pause-to-investigation events and TST immobility time in controls and bystanders that received foot shocks (linear regression, $n_{BYFs\text{-}saline}$ = 12, $n_{BYFs\text{-}PCPA}$ = 11, BY-Fs saline R^2 = 0.3526, P = 0.0418, BY-Fs PCPA R^2 = 0.0378, P = 0.5667). Error bars represent mean ± SEM or median ± min-to-max whiskers.

para-chlorophenylalanine (PCPA, three intraperitoneal injections of 200 mg/kg) (*22*) prevented NEC reduction of LHb neuronal bursting (Fig. 3, I to K, and fig. S5, K to M).

Modulation of behavioral despair by 5-HT manipulation

Given that NEC promotes resilience and habenular 5-HT release, we wondered whether manipulating 5-HT release in the LHb is sufficient and necessary for controlling the mouse emotional responsivity. We expressed Cre-dependent ChRimson-tdTomato or tdTomato

(control) in raphe 5-HT neurons of Sert-Cre mice (Fig. 4A). Optically activating 5-HT inputs (10-ms pulses at 10 Hz for 10 min) in the LHb, which emulates increased 5-HT during NEC, reduced LHb neuronal bursting (Fig. 4, B and C, and fig. S6, A to C). When the same protocol was applied before the adverse experience, it promoted resilience, precluding the expression of behavioral despair and thereby recapitulating the resilient phenotype after NEC (Fig. 4, D and E). The high level of immobility in the TST (i.e., behavioral despair) was instead the phenotype present in mice injected with a control virus and exposed to adverse conditions (Fig. 4, D and E). Next, we tested whether silencing 5-HT release would impair the resilient phenotype produced by NEC. We expressed a targeting-enhanced mosquito homolog of the vertebrate encephalopsin (eOPN3) that is temporally effective in suppressing presynaptic transmission (*23*). Disrupting 5-HT release throughout the NEC task (0.2 Hz for 1 s; see methods) reduced bystanders' pausing during NEC, consequently leading to the expression of behavioral despair after an adverse experience (Fig. 4, G and H, and fig. S6D). Moreover, the immobility in the TST correlated with pause-to-investigation transitions and pausing time in 5-HT^{tdTomato} but not in 5-HT^{eOPN3} bystander mice (Fig. 4I and fig. S6E). Pharmacologically depleting 5-HT with PCPA also disrupted the relationship between the behavioral phenotypes during NEC and despair after an adverse experience, further corroborating these observations (Fig. 4, J and K, and fig. S6F).

Discussion

A plasticity mechanism in the habenula thus emerges as underlying an unprecedented modulatory role of 5-HT for resilience. In naïve mice, detrimental experiences including exposure to persistent inescapable foot shock or stress lead to depressive-like symptoms including behavioral despair (*24*). We demonstrated that in bystander mice, the transfer of negative emotions adjusts their affective state to cope with subsequent adverse experiences, thus leading to a resilient phenotype. Such behavioral remodeling requires enhanced 5-HT release in the LHb, which in turn reduces the discrete neuronal activity pattern of neuronal bursting.

We propose a neural mechanism occurring during a rapid observational experience in mice that results in an efficient transfer of emotions, referred to here as negative emotional contagion (*5*). Whether negative emotional contagion emerges after witnessing adverse experiences other than foot shocks remains to be addressed. Social contagion between individuals extends across diverse modalities, including food safety, pain, learning (*6*, *25*, *26*), and, as shown here, affective state. Indeed, bystanders can acquire various behaviors from demonstrators, ranging from food and shock avoidance to pain reaction (*6*, *25*, *26*), but remain shielded from developing behavioral despair. The bystander mice exhibit potential facets of empathy: (i) they integrate information about another's affective state and (ii) they display social interest (i.e., investigation increases during the task) (*26*, *27*). As a consequence, these empathy-like features may likely favor coping behaviors over vulnerability to adversity (*28*). Our data provide a complementary aspect to the framework of social contagion, that is, the protection from the emergence of negative affect (behavioral despair) likely enhancing the fitness of individuals. These findings support the notion that, as is the case in humans, graded trauma can promote resilience, enabling individuals to cope with future challenges (*2*, *3*, *29*, *30*).

The negative emotional contagion task modulates LHb function. To date, the accepted model proposes that adverse experience promotes habenular hyperactivity and enhanced bursting, causing depressive-like symptoms (*12*, *21*, *31*, *32*). The findings here describe the capacity of a vicarious affective experience to lessen LHb burst activity. This suggests that neuronal activity in the LHb moves along the individuals' emotional gradient, whereby indirect and nonphysical experience lowers bursting and thus promotes resilience, whereas direct physical adverse conditions boost LHb firing, promoting despair. These findings expand the clinical implication of LHb neuronal activity by suggesting that the emergence of depressive-like symptoms can be both limited and reversed by manipulating LHb bursting (*21*).

The contribution of 5-HT release during negative emotional contagion in promoting resilience through the reduction in LHb burst activity is in line with the demonstration that 5-HT reduces synaptic excitation onto LHb neurons (*17*, *33*–*35*). Although this suggests that one feature of 5-HT is to diminish LHb synaptic function and activity, it only partly covers the many repercussions that 5-HT release has on the LHb. Ex vivo and in vivo recordings indicate that 5-HT increases neuronal excitability and reduces presynaptic γ-aminobutyric acid release (*18*, *33*, *36*). In addition, 5-HT terminals from the raphe, concomitantly with 5-HT, could co-release glutamate (*37*, *38*). Thus, manipulation of 5-HT terminals may modulate bursting through fast or volume neurotransmission. Related to 5-HT neuromodulation, pharmacological and transcriptomic data from LHb cells identify several 5-HT receptors, including the 1, 2c, and 5b subtypes (*16*, *39*, *40*). Acting on metabotropic receptors, 5-HT may modulate intrinsic conductances, which are shown to be relevant for LHb bursting (*21*, *41*). Understanding the circuit-specific localization of such receptors, their function in modulating LHb activity, and the repercussions on LHb targets and behaviors are important matters for future studies.

The present behavioral and mechanistic investigation expands the understanding of neuromodulatory signaling that controls the affective state and how monoamines influence habenular circuits (*42*–*44*). This may open new therapeutically relevant applications combining the study of the serotonergic system and novel pharmacological 5-HT actuators (psychedelics, for instance) in the context of psychiatry (*45*). In summary, 5-HT release resets the individuals' emotional state to face adverse conditions by acting on key neuronal circuits and activity modalities, thereby refining the current circuit model for depression.

REFERENCES AND NOTES

1. C. Faye, J. C. Mcgowan, C. A. Denny, D. J. David, *Curr. Neuropharmacol.* **16**, 234–270 (2018).
2. R. Kalisch, S. J. Russo, M. B. Müller, *Physiol. Rev.* **104**, 1205–1263 (2024).
3. S. J. Russo, J. W. Murrough, M. H. Han, D. S. Charney, E. J. Nestler, *Nat. Neurosci.* **15**, 1475–1484 (2012).
4. E. J. Nestler, S. J. Russo, *Neuron* **112**, 1911–1929 (2024).
5. C. Keysers, V. Gazzola, *Affect. Sci.* **4**, 662–671 (2023).
6. S. A. Allsop *et al*., *Cell* **173**, 1329–1342.e18 (2018).
7. P. Atsak *et al*., *PLOS ONE* **6**, e21855 (2011).
8. C. Keysers, V. Gazzola, *Curr. Biol.* **31**, R728–R730 (2021).
9. S. E. Silverstein *et al*., *Nature* **626**, 1066–1072 (2024).
10. H. Hu, Y. Cui, Y. Yang, *Nat. Rev. Neurosci.* **21**, 277–295 (2020).
11. S. Lecca, F. J. Meye, M. Mameli, *Eur. J. Neurosci.* **39**, 1170–1178 (2014).
12. S. Lecca *et al*., *Nat. Med.* **22**, 254–261 (2016).
13. S. Ma *et al*., *Nature* **622**, 802–809 (2023).
14. R. P. Vertes, W. J. Fortin, A. M. Crane, *J. Comp. Neurol.* **407**, 555–582 (1999).
15. D. F. Cardozo Pinto *et al*., *Nat. Commun.* **10**, 4633 (2019).
16. M. E. Flanigan *et al*., *Nat. Commun.* **14**, 1800 (2023).
17. S. J. Shabel, C. D. Proulx, A. Trias, R. T. Murphy, R. Malinow, *Neuron* **74**, 475–481 (2012).
18. S. J. Shabel, C. D. Proulx, J. Piriz, R. Malinow, *Science* **345**, 1494–1498 (2014).
19. I. Pollak Dorocic *et al*., *Neuron* **83**, 663–678 (2014).
20. F. Deng *et al*., *Nat. Methods* **21**, 692–702 (2024).
21. Y. Yang *et al*., *Nature* **554**, 317–322 (2018).
22. H. C. Dringenberg, E. L. Hargreaves, G. B. Baker, R. K. Cooley, C. H. Vanderwolf, *Behav. Brain Res.* **68**, 229–237 (1995).
23. M. Mahn *et al*., *Neuron* **109**, 1621–1635.e8 (2021).
24. S. J. Russo, E. J. Nestler, *Nat. Rev. Neurosci.* **14**, 609–625 (2013).
25. M. Loureiro *et al*., *Science* **364**, 991–995 (2019).
26. M. L. Smith, N. Asada, R. C. Malenka, *Science* **371**, 153–159 (2021).
27. J. B. Panksepp, G. P. Lahvis, *Neurosci. Biobehav. Rev.* **35**, 1864–1875 (2011).
28. A. Olsson, V. Spring, in *Neuronal Correlates of Empathy: From Rodent to Human*, K. Meyza, E. Knapska, Eds. (Elsevier Academic Press, 2018), pp. 7–23.
29. A. D. Mancini, *Psychol. Rev.* **126**, 486–505 (2019).
30. M. D. Seery, E. A. Holman, R. C. Silver, *J. Pers. Soc. Psychol.* **99**, 1025–1041 (2010).
31. I. Cerniauskas *et al*., *Neuron* **104**, 899–915.e8 (2019).
32. B. Li *et al*., *Nature* **470**, 535–539 (2011).
33. F. Delicata *et al*., *CNS Neurosci. Ther.* **24**, 721–733 (2018).
34. G. Xie *et al*., *Sci. Rep.* **6**, 23798 (2016).
35. H. Zhang *et al*., *Brain Struct. Funct.* **223**, 2243–2258 (2018).
36. W. Zuo *et al*., *Neuropharmacology* **101**, 449–459 (2016).
37. J. Ren *et al*., *eLife* **8**, e49424 (2019).
38. C. Sego *et al*., *J. Comp. Neurol.* **522**, 1454–1484 (2014).
39. Y. Hashikawa *et al*., *Neuron* **106**, 743–758.e5 (2020).
40. M. L. Wallace *et al*., *eLife* **9**, e51271 (2020).
41. M. Noda, H. Higashida, S. Aoki, K. Wada, *Mol. Neurobiol.* **29**, 31–39 (2004).
42. S. Lammel *et al*., *Neuron* **85**, 429–438 (2015).
43. A. M. Stamatakis *et al*., *Neuron* **80**, 1039–1053 (2013).
44. L. Michel, P. Molina, M. Mameli, *Neuron* **112**, 2669–2685 (2024).

45. B. D. Heifets, R. C. Malenka, *JAMA Psychiatry* **76**, 775–776 (2019).
46. S. Mondoloni, M. Mameli, Emotional contagion, habenula, and serotonin, version v1, Zenodo (2024); https://doi.org/10.5281/zenodo.12179865.

ACKNOWLEDGMENTS

We thank M. Diana, E. Schwartz, J. Graff, and all the members of the Mameli laboratory for their comments on the manuscript. We thank L. Restivo for support in behavioral experiment design and analysis as well as L. Zweifel for the constructive discussions on the project. **Funding:** The Swiss National Science Foundation 31003A-175549 (M.M.); the Swiss State Secretariat for Education, Research and Innovation SVEN (M.M.); the Canton of Vaud (M.M.). **Author contributions:** Conceptualization: S.M. and M.M. Methodology: S.M., F.D., Y.L., M.F., T.K., M.M., and D.O. Investigation: S.M., P.M., F.C., S.L., A.L.L., M.C., M.F., C.-H.W., and L.M. Visualization: S.M. and M.M. Funding acquisition: M.M. Project administration: S.M. and M.M. Supervision: M.M. and S.M. Writing – original draft: S.M. and M.M. Writing – review & editing: S.M., M.M., P.M., S.L., A.L.L., M.C., T.K., M.F., and Y.L. **Competing interests:** The authors declare that they have no competing interests. **Data and materials availability:** All data are available in the main text or supplementary materials and deposited at Zenodo (*46*). This research was funded in whole or in part by the Swiss National Science Foundation (31003A-175549), a cOAlition S organization. The author will make the Author Accepted Manuscript (AAM) version available under a CC BY public copyright license.

SUPPLEMENTARY MATERIALS

science.org/doi/10.1126/science.adp3897
Materials and Methods
Supplementary Text
Figs. S1 to S6
MDAR Reproducibility Checklist

Submitted 22 March 2024; accepted 8 July 2024
10.1126/science.adp3897